minerals

MDPI

Article

LKZ-1: A New Zircon Working Standard for the In Situ Determination of U–Pb Age, O–Hf Isotopes, and Trace Element Composition

Albert Chang-sik Cheong [1,*], Youn-Joong Jeong [1], Shinae Lee [1], Keewook Yi [1], Hui Je Jo [2], Ho-Sun Lee [3], Changkun Park [4], Nak Kyu Kim [4], Xian-Hua Li [5] and Sandra L. Kamo [6]

1 Korea Basic Science Institute, Cheongju 28119, Korea; hero0123@kbsi.re.kr (Y.-J.J.); lsa2011@kbsi.re.kr (S.L.); kyi@kbsi.re.kr (K.Y.)
2 Korea Institute of Geoscience and Mineral Resources, Daejeon 34132, Korea; jhj8218@kigam.re.kr
3 Core Research Facilities, Pusan National University, Busan 46241, Korea; geosun@pusan.ac.kr
4 Korea Polar Research Institute, Incheon 21990, Korea; changkun@kopri.re.kr (C.P.); kimnk@kopri.re.kr (N.K.K.)
5 Institute of Geology and Geophysics, Chinese Academy of Sciences, Beijing 100027, China; lixh@gig.ac.cn
6 Jack Satterly Geochronology Laboratory, University of Toronto, Toronto, ON M5S 3B1, Canada; skamo@es.utoronto.ca
* Correspondence: ccs@kbsi.re.kr; Tel.: +82-43-240-5170

Received: 3 April 2019; Accepted: 24 May 2019; Published: 27 May 2019

Abstract: This study introduces a new zircon reference material, LKZ-1, for the in situ U–Pb dating and O–Hf isotopic and trace element analyses. The secondary ion mass spectrometric analyses for this gem-quality single-crystal zircon yielded a weighted mean $^{206}Pb/^{238}U$ age of 572.6 ± 2.0 Ma (2σ, n = 22, MSWD = 0.90), with moderately high U concentrations (619 ± 21 ppm, 1 SD), restricted Th/U ratios (0.146 ± 0.002, 1 SD), and negligible common Pb content ($^{206}Pb_c$ < 0.2%). A comparable $^{206}Pb/^{238}U$ age (570.0 ± 2.5 Ma, 2σ) was produced by the isotope dilution-thermal ionization mass spectrometry. The secondary ion mass spectrometric and laser ablation-assisted multiple collector inductively coupled plasma mass spectrometer analyses respectively showed that LKZ-1 had little variation in O ($\delta^{18}O_{V\text{-}SMOW}$ = 10.65 ± 0.14‰; laser fluorination value = 10.72 ± 0.02‰; 1 SD) and Hf ($^{176}Hf/^{177}Hf$ = 0.281794 ± 0.000016, 1 SD) isotopic compositions. LKZ-1 was also fairly homogeneous in its chemical composition (RSD of laser ablation ICPMS data ≤ 10%), displaying a relatively uniform chondrite-normalized rare earth element pattern ($(Lu/Gd)_N$ = 31 ± 3, Eu/Eu^* = 0.43 ± 0.17, Ce/Ce^* = 44 ± 32; 1 SD). These consistencies suggest that the LKZ-1 zircon is a suitable working standard for geochronological and geochemical analyses.

Keywords: zircon; working standard; LKZ-1; U–Pb age; O isotopes; Hf isotopes; trace element

1. Introduction

Geochemical and geochronological data for rocks and minerals have long been obtained by wet chemical and isotopic analyses [1,2]. Despite the constraints of time-consuming and labor-intensive sample preparation, wet analysis is still widely used, particularly when a high level of precision is demanded. However, if the sample is composed of chemically or isotopically heterogeneous domains that have their own petrogenetic significance, microsampling strategies are inevitably required.

Technical advances during the past several decades have facilitated the routine analysis of tiny single crystals at the subgrain scale. The high spatial resolution of microbeam techniques, typically of the micrometer- or submicrometer-scale [3,4], provides an excellent opportunity to integrate the chemical and isotopic data from individual subgrain domains with textural observations (e.g., [5]). Zircon

($ZrSiO_4$) has been a prime target of in situ analysis using secondary ion mass spectrometry (SIMS) [6,7] or laser ablation (LA)-assisted inductively coupled plasma mass spectrometry (ICPMS) [8,9], mainly for its ability to retain the original isotopic signature due to its strong resistance to physicochemical breakdown and slow intracrystalline diffusion of constituent ions [10]. Zircon can provide U–Pb age constraints, as well as trace element and O–Hf isotope data for given microdomains. The integration of such multifaceted zircon data has proven to be a powerful tool for addressing the diverse issues related to crustal evolution [11–14].

Microbeam analysis can be performed rapidly and requires minimal sample preparation; however, the measured data should be carefully corrected and calibrated for spectral and isobaric interference and instrumental fractionation. This process is generally achieved using matrix-matched standards, which are used as a reference material to check the data accuracy and, more importantly, as a primary standard to calculate the inter-elemental isotope ratios or instrumental mass fractionation (IMF) factors. In the latter case, the relative isotopic composition of the standard should be uniform and accurately known, because it directly affects the results calculated for unknown samples. Many zircon standards have been suggested for U–Th–Pb dating and chemical/isotopic analyses. Among these, 91500 [15], FC1 [16], Temora [17,18], and Plešovice [19] are widely used; however, their supply is quite limited. For example, the International Association of Geoanalysts provides only a limited amount of zircon 91500 per laboratory, with the recommendation that it be used initially to establish an in-house reference material. It is also noted that some zircon standards are chemically inhomogeneous [19,20]. Thus, there is still demand for high-quality zircon standards.

This study introduces a new zircon reference material LKZ-1. We measured its U–Pb age and Hf isotopic composition using a high-resolution (HR)-SIMS, isotope dilution thermal ionization mass spectrometry (ID-TIMS), and LA-multiple collector (MC)-ICPMS. The oxygen isotopic composition of LKZ-1 was measured using a laser fluorination system and HR-SIMS. The chemical composition of LKZ-1 was measured using a quadrupole ICPMS connected to a femtosecond LA system.

2. Materials and Methods

2.1. LKZ-1

LKZ-1 is a single transparent pale yellow megacryst of gem-quality zircon with no visible inclusions or cracks (Figure 1). The total mass was 0.83 g. The LKZ-1 was imported from Sri Lanka by an online gem dealer and purchased by the Korea Basic Science Institute (KBSI) in 2014. No information about the nature of its host rock is available.

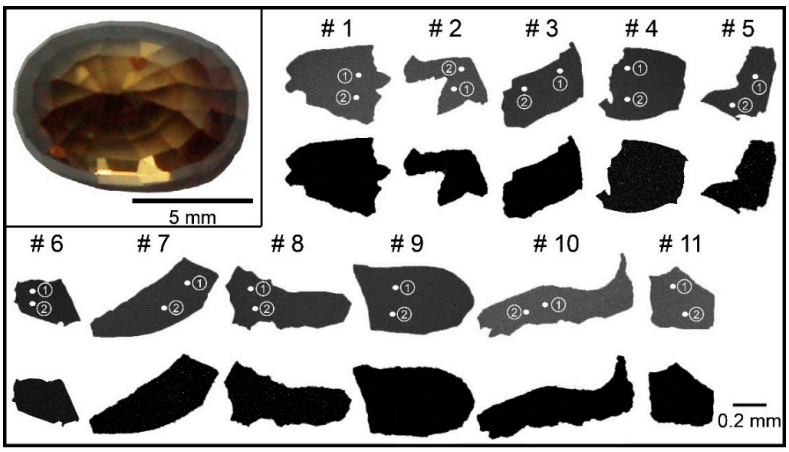

Figure 1. A photograph of the LKZ-1 zircon (inset) and representative backscattered electron (upper) and cathodoluminescence (lower) images. The grain and spot numbers are the same as in Table 2.

Our previous LA-MC-ICPMS analyses confirmed that this zircon is in a ^{238}U–^{230}Th radioactive equilibrium [21]. It is noted that the preliminary ion microprobe U–Pb data for LKZ-1, presented by Kim et al. (2015) [22], are revised in this study.

2.2. HR-SIMS U–Pb Analysis

Fragments of the LKZ-1 zircon were mounted in epoxy with reference zircons for in situ isotopic and chemical analyses. The U–Th–Pb isotopic analyses were conducted using a sensitive high-resolution ion microprobe (SHRIMP IIe/MC) at the KBSI Ochang Center. Before the SHRIMP analyses, cathodoluminescence (CL) and backscattered electron (BSE) images of the fragments were examined using a scanning electron microscope (SEM) (JEOL JSM-6610LV). The primary O_2^- beam was focused into a ~25-μm-diameter spot at an accelerating voltage of 10 kV. The collector slit width was fixed at 100 μm, achieving a mass resolution of about 5000 at 1% peak height. We used the 91500 ($^{206}Pb/^{238}U$ age = 1062.4 Ma, [15]) and SL13 (U = 238 ppm) standard zircons for Pb/U calibration and to determine the U abundance, respectively. The Pb/U ratios were calibrated against the 91500 zircon according to the power law relationship between Pb^+/U^+ and UO^+/U^+. The Th/U ratios were estimated using a fractionation factor derived from the measured $^{232}Th^{16}O^+/^{238}U^{16}O^+$ versus $^{208}Pb/^{206}Pb$ of the SL13 standard. The common Pb was corrected using the ^{207}Pb method [23]. Data processing was conducted using the SQUID 2.50 and Isoplot 3.75 software [24,25]. The weighted mean ages were calculated after excluding the outliers using the Student's t-test and reported at the 95% confidence level.

2.3. ID-TIMS U–Pb Analysis

ID-TIMS U–Pb isotopic analyses were performed at the Jack Satterly Geochronology Laboratory in the Department of Earth Sciences, University of Toronto (Toronto, ON, Canada). Four fragments were selected for analyses. The fragments were chemically abraded prior to dissolution [26]. This process involved thermal annealing in a muffle furnace at 900 °C for 48 h followed by a chemical etch for 9 h in ~0.10 mL concentrated hydrofluoric acid and ~10 μL 8N nitric acid in Teflon dissolution vessels at 200 °C. The fragments were rinsed with distilled water, and washed in 8N HNO_3. A mixed ^{205}Pb–^{235}U spike was added to the Teflon dissolution capsules during sample loading. The zircon-spike mixture was dissolved using ~0.10 mL concentrated hydrofluoric acid and ~0.02 mL 8N nitric acid at 200 °C [27] for 5 days, dried to a precipitate, and re-dissolved in ~0.15 mL 3N hydrochloric acid. The U and Pb were isolated from the zircon solutions using anion exchange chromatography, dried in dilute phosphoric acid, and deposited onto outgassed rhenium filaments with silica gel [28]. The U and Pb were analyzed using a VG M354 mass spectrometer with multiple Faraday collectors in static mode for Pb and a single Daly pulse-counting system in dynamic mode for U measurements. The dead time of the Daly measuring system for U was 14.5 ns. The mass discrimination correction for the Daly detector was constant at 0.03%/atomic mass unit. The amplifier gains and Daly characteristics were monitored using the SRM 982 Pb standard. A thermal mass fractionation correction of 0.1(±0.05)% per atomic mass unit for Pb and U was applied. The total common Pb in each zircon analysis was assumed to have the isotopic composition of laboratory blank ($^{206}Pb/^{204}Pb$ = 18.49 ± 0.4%; $^{207}Pb/^{204}Pb$ = 15.59 ± 0.4%; $^{208}Pb/^{204}Pb$ = 39.36 ± 0.4%). The total amount of common Pb in the present analyses ranged from 0.5 to 4.7 picograms. The Pb/U and Pb/Pb isotopic ratios were corrected for IMF, common Pb in the spike, and blank. The Th/U ratios were calculated from the radiogenic $^{208}Pb/^{206}Pb$ ratio and $^{207}Pb/^{206}Pb$ age assuming concordance. Corrections for ^{230}Th disequilibrium in $^{206}Pb/^{238}U$ and $^{207}Pb/^{206}Pb$ were made assuming Th/U of 4.2 in the magma. We used the decay constants of Jaffey et al. (1971) [29] (^{238}U and ^{235}U are 1.55125×10^{-10} and 9.8485×10^{-10} per year, respectively). The $^{238}U/^{235}U$ ratio of 137.88 was used for the $^{207}Pb/^{206}Pb$ model age calculations. All the age errors quoted in the text and table, and error ellipses in the concordia diagram are given at 2σ. Plotting and age calculations were obtained using the Isoplot/Ex 3.00 software [30].

2.4. Oxygen Isotope Analysis

Zircon oxygen isotopes were measured using a laser fluorination system at the Korea Polar Research Institute (KOPRI), and the Cameca IMS 1280 ion probe at the SIMS laboratory of the Institute of Geology and Geophysics, Chinese Academy of Sciences (CAS) in Beijing, China.

The laser fluorination system at the KOPRI for oxygen isotopic analysis is well described elsewhere [31]. About 3 mg of the LKZ-1 zircon was loaded in the nickel sample holder, and then the sample holder was placed in the reaction chamber. The chamber that was assembled with a purification line was evacuated to 10^{-3} mbar or better, and heated for over 10 h by an external heater to eliminate the absorbed moisture inside the chamber. Before the sample was analysed, the chamber was pre-fluorinated by a small amount of BrF_5 for 1 h at room temperature to completely remove the moisture absorbed on the sample surfaces and inside the chamber. Any remaining gases in the reaction chamber were thoroughly evacuated by a diffusion pump ($<10^{-4}$ mbar), and then sufficient BrF_5 was introduced into the chamber for laser fluorination of the sample. The sample was gradually heated using a defocused CO_2 infrared laser beam by automatically increasing the lasing power up to 60%. All the gaseous species derived from the samples were introduced into the purification line consisting of two cryogenic traps (liquid nitrogen, −196 °C) and a heated KBr getter. A molecular sieve (MS13X) pellet on the final cryogenic trap collected the pure O_2 for 10 min at liquid nitrogen temperature. The oxygen yield of the sample was calculated by the pressure value of the recovered O_2 gas from MS13X. The oxygen isotopic composition of the sample gas was analyzed using a dual-inlet isotope ratio mass spectrometer (MAT 253 Plus, Thermo Fisher Scientific, Waltham, MA, USA) connected on-line to the laser fluorination system. The measured $^{18}O/^{16}O$ ratios were normalized to the Vienna standard mean oceanic water (V-SMOW) ($^{18}O/^{16}O$ = 0.0020052, [32]) and presented as $\delta^{18}O$ notation. The long-term reproducibility of the laser fluorination system based on the repeated analyses (n = 28) of in-house obsidian standard is ±0.08‰ (1σ) for $\delta^{18}O$ [31].

For the SIMS analyses at the CAS, the Gaussian focused Cs^+ primary ion beam was accelerated at 10 kV, with an intensity of ~1.6 nA. The spot size was approximately 20 μm in diameter (10 μm beam + 10 μm raster). A normal incidence electron flood gun was used to compensate for sample charging. The magnetic field was stabilized using a nuclear magnetic resonance controller. Negative secondary ions were extracted with a potential of −10 kV. The field aperture was 6000 × 6000 μm^2. A ~120 μm entrance slit, 40 eV energy slit, ~133 transfer magnification, and 500 μm exit slit provided a mass resolution of ~2500 at 1% peak height. Under these conditions, the count rate of $^{16}O^-$ was typically ~1×10^9 cps/nA. The ^{16}O and ^{18}O ions were detected simultaneously using two Faraday cups with 10^{10} and 10^{11} Ω resistors, respectively. The in-run precision was typically better than 0.2 ‰ (2 standard errors). The IMF was corrected based on the 91500 zircon value suggested by Valley (2003) [7] ($\delta^{18}O_{V\text{-}SMOW}$ = 10.07 ± 0.03‰).

2.5. LA-MC-ICPMS U–Pb and Lu–Yb–Hf Isotope Analysis

Zircon U–Pb and Lu–Yb–Hf isotopes were measured using a Plasma II MC-ICPMS (Nu Instruments) equipped with an NWR193-nm ArF Excimer laser ablation system at the KBSI Ochang Center. The instrumental parameters for the U–Pb and Lu–Yb–Hf isotopic analyses are summarized in Table 1. The raw data were processed using Iolite 2.5 within the Igor Pro 6.3.5.5 software [33], and corrected for the background. The instrumental mass discrimination and laser-induced elemental fractionation during the U–Pb analysis were corrected by calibration against the 91500 zircon. No common Pb correction was performed. The ages were calculated using the Isoplot 3.75 software [25]. All the ratios were calculated with 2σ errors.

Table 1. LA-MC-ICPMS instrument and operational parameters for U–Pb dating and Lu–Yb–Hf isotope analysis.

Parameter	U–Pb	Lu–Yb–Hf
	MC-ICPMS	
Instrument	Nu Plasma II	
RF power	1300 W	1300 W
Reflected power	<1 W	<1 W
Mixed gas & flow rate	Ar, ~0.9 L/min	Ar, ~0.7 L/min
Auxiliary gas & flow rate	Ar, 0.9 L/min	Ar, 0.9 L/min
Cool gas & flow rate	Ar, 13 L/min	Ar, 13 L/min
Sampler cone	Ni (1 mm orifice)	Ni (1 mm orifice)
Skimmer cone	Ni (0.7 mm orifice)	Ni (0.7 mm orifice)
Data acquisition mode	Time resolved analysis	Time resolved analysis
Integration time	0.2 s	0.2 s
Collectors	2 Faraday cups and 5 ion counters	10 Faraday cups
Measured isotopes	^{238}U, ^{232}Th, ^{208}Pb, ^{207}Pb, ^{206}Pb, ^{204}Pb, ^{202}Hg	^{172}Yb, ^{173}Yb, ^{174}(Hf + Yb), ^{175}Lu, ^{176}(Hf + Yb + Lu), ^{177}Hf, ^{178}Hf, ^{179}Hf, ^{180}Hf, ^{183}W
Laser ablation system		
Laser	ESI machines 193nm ArF excimer laser	
Ablation mode	Single hole drilling	
Cell	Two volume 2 cell (10 × 10 cm)	
Sample transport tubing	0.5 m length	0.5m length
Pulse repetition rate & width	5Hz, <4 ns	10Hz, <4 ns
Pulse energy density	~3 J/cm^2	~ 8 J/cm^2
Ablation duration	30 s	60 s
Carrier gas & flow rate	He, 0.65 L/min	He, 0.65 L/min; N_2, 0.002 L/min
Crater size	~15 μm	~50 μm
Drill depth	~4 μm	~20 μm

The ^{176}Lu and ^{176}Yb interferences on the ^{176}Hf signal were corrected using the isotopic values suggested by Chu et al. (2002) [34] and Vervoort et al. (2004) [35], respectively, on the basis of previous MC-ICPMS results for mixed standard solutions [36]. The mass bias of the measured Hf isotopic ratios was corrected to ^{179}Hf/^{177}Hf = 0.7325 using an exponential correction law. The ^{176}Lu/^{177}Hf and ^{176}Yb/^{177}Hf ratios were calculated following the method of Iizuka and Hirata (2005) [37]. The ε_{Hf} values were calculated using a ^{176}Lu decay constant of 1.865×10^{-11} per year [38] and the chondritic values suggested by Blichert-Toft and Albarède (1997) [39].

2.6. LA-Quadrupole ICPMS Analysis

The minor and trace elements were analyzed using a 343 nm femtosecond laser ablation microprobe (J200 LA model, Applied Spectra Inc., Fremont, CA, USA) coupled to an iCapQ model (Thermo Fisher Scientific, Bremen, Germany) quadrupole ICPMS at the Core Research Facilities, Pusan National University, Korea. The zircon surfaces were ablated at a pulse repetition rate of 10 Hz and a pulse energy of 250 μJ, producing a ~30-μm-diameter crater pit. Helium (700 mL/min) was flushed into the sample cell to increase the sample transport efficiency and reduce aerosol deposition around the ablation pit [40]. The instrumental parameters of ICPMS were optimized to provide the highest sensitivity, whilst maintaining the ratio of ThO^+/Th^+ below 0.005. The zircon data were externally calibrated using NIST 610 standard glass, and internally normalized using ^{29}Si and ^{91}Zr. The reference values for the NIST 610 were taken from Jochum et al. (2011) [41], and the stoichiometric values of zircon (Si = 15.3%, Zr = 47.6%) were used for normalization.

3. Results and Discussion

3.1. U–Pb Age

As shown in Figure 1, the LKZ-1 fragments were relatively dark under CL. The CL and BSE images showed no clear zonation patterns. The HR-SIMS (SHRIMP) U–Th–Pb isotope data are presented

in Table 2. The common Pb proportion in ^{206}Pb, calculated using the ^{204}Pb counts and an assumed Pb isotopic composition after the model of Stacey and Kramers (1975) [42], was mostly less than 0.1%. The SHRIMP analyses produced consistently concordant data (Figure 2). The ^{207}Pb-corrected data generated a weighted mean ^{206}Pb/^{238}U age of 572.6 ± 2.0 Ma (n = 22, MSWD = 0.90), which was consistent with the ^{204}Pb-corrected ^{207}Pb/^{206}Pb age (weighted mean = 573 ± 12 Ma, n = 21, MSWD = 1.4). The relatively uniform concentrations of U (619 ± 21 ppm, 1 standard deviation, same hereafter unless otherwise stated) and Th (90.2 ± 4.2 ppm) yielded highly consistent Th/U ratios of 0.146 ± 0.002. The Plešovice zircon (ID-TIMS ^{206}Pb/^{238}U age = 337.13 ± 0.37 Ma; [19]), analyzed together with LKZ-1, yielded a weighted mean ^{206}Pb/^{238}U age of 338.7 ± 1.4 Ma (n = 15, MSWD = 0.81) (Table S1).

Table 2. SHRIMP U–Th–Pb results for the LKZ-1 zircon.

Spot No.	^{206}Pbc[1] (%)	^{206}Pb/^{238}U[2]	±%	^{207}Pb/^{206}Pb[2]	±%	Th (ppm)	U (ppm)	Disc.%	Date[3] (Ma)		
LKZ_1.1	0.01	0.2322	2.62	0.0590	0.84	97.4	652	−1.1	570.3	±	4.5
LKZ_1.2	0.04	0.2310	3.17	0.0595	0.85	93.4	636	0.6	569.1	±	4.5
LKZ_2.1	0.13	0.2220	0.45	0.0592	0.88	87.0	603	−6.3	565.7	±	9.4
LKZ_2.2	0.07	0.2157	2.50	0.0590	0.89	87.7	607	−3.8	566.9	±	4.5
LKZ_3.1	0.05	0.2227	2.80	0.0600	0.87	90.3	619	2.7	572.5	±	4.6
LKZ_3.2	0.07	0.2299	1.86	0.0591	2.31	86.3	597	−3.7	572.2	±	4.6
LKZ_4.1	0.06	0.2272	1.53	0.0602	0.86	92.4	626	3.2	572.4	±	4.6
LKZ_4.2	0.01	0.2210	2.11	0.0603	0.88	92.6	631	6.4	570.5	±	4.5
LKZ_5.1		0.2248	1.42	0.0587	0.89	90.3	621	−3.8	580.8	±	4.7
LKZ_5.2		0.2189	1.76	0.0584	0.89	90.3	627	−5.9	577.8	±	4.6
LKZ_6.1		0.2224	2.14	0.0600	0.88	89.1	619	8.3	568.0	±	4.5
LKZ_6.2		0.2185	0.45	0.0591	0.89	96.3	656	1.1	580.1	±	4.6
LKZ_7.1	0.07	0.2261	1.90	0.0593	1.55	82.0	576	−2.8	573.4	±	4.6
LKZ_7.2	0.08	0.2294	1.41	0.0599	0.89	86.4	599	0.0	574.3	±	4.6
LKZ_8.1	0.16	0.2272	1.78	0.0587	1.69	89.7	620	−15.1	580.0	±	6.8
LKZ_8.2	0.03	0.2228	1.98	0.0583	0.91	89.8	619	−9.2	580.9	±	7.8
LKZ_9.1	0.01	0.2261	1.76	0.0586	0.91	85.4	598	−4.6	572.6	±	4.6
LKZ_9.2		0.2245	2.20	0.0587	1.57	86.8	607	−3.6	578.7	±	4.7
LKZ_10.1		0.2275	2.00	0.0598	0.85	96.8	649	6.2	571.1	±	4.6
LKZ_10.2	0.02	0.2303	2.05	0.0596	0.85	97.7	652	2.0	570.2	±	4.6
LKZ_11.1		0.2313	1.84	0.0593	0.88	87.7	602	3.8	564.7	±	4.6
LKZ_11.2	0.07	0.2297	1.72	0.0572	0.99	89.3	608	−19.7	571.3	±	4.6

[1] ^{204}Pb-based common ^{206}Pb proportion; [2] Uncorrected data; [3] ^{207}Pb-corrected ^{206}Pb/^{238}U date.

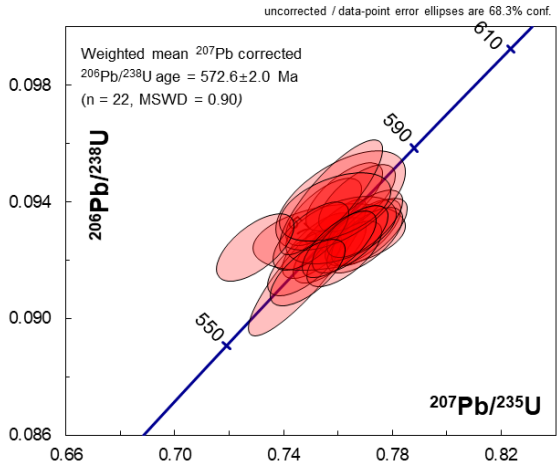

Figure 2. ^{206}Pb/^{238}U-^{207}Pb/^{235}U concordia diagram showing the SHRIMP results for the LKZ-1 zircon with ±1σ error ellipses. The plotted data are uncorrected for common Pb.

The LA-MC-ICPMS U–Pb results for the LKZ-1 zircon are listed in Table 3, and shown graphically in Figure 3. The LA-MC-ICPMS analyses produced concordant age data, with a weighted mean ^{206}Pb/^{238}U age of 574.8 ± 1.3 Ma (n = 28, MSWD = 1.13).

Table 3. LA-MC-ICPMS U–Pb results for the LKZ-1 zircon.

Spot No.	$^{206}Pb/^{238}U$	2SE	Date (Ma)	2SE	$^{207}Pb/^{206}Pb$	2SE	Date (Ma)	2SE
LKZ-1-1	0.0929	0.0011	574.1	6.6	0.0594	0.0006	580	11
LKZ-1-2	0.0934	0.0011	575.6	6.2	0.0589	0.0007	562	17
LKZ-1-3	0.0931	0.0008	573.9	4.7	0.0593	0.0005	571	10
LKZ-1-4	0.0928	0.0013	572.2	7.7	0.0592	0.0007	564	13
LKZ-1-5	0.0924	0.0008	569.8	4.6	0.0589	0.0005	566	12
LKZ-1-6	0.0942	0.0013	580.4	7.8	0.0589	0.0005	566	10
LKZ-1-7	0.0935	0.0013	576.9	7.5	0.0592	0.0005	572	10
LKZ-1-8	0.0943	0.0014	581.0	8.0	0.0589	0.0005	568	10
LKZ-1-9	0.0944	0.0015	581.4	9.0	0.0588	0.0005	559	11
LKZ-1-10	0.0937	0.0015	577.9	8.7	0.0587	0.0004	555	9
LKZ-1-11	0.0935	0.0015	576.1	8.6	0.0587	0.0005	559	11
LKZ-1-12	0.0923	0.0013	569.1	7.9	0.0587	0.0005	553	11
LKZ-1-13	0.0932	0.0015	574.3	8.9	0.0589	0.0005	561	12
LKZ-1-14	0.0923	0.0013	568.8	7.5	0.0585	0.0006	547	12
LKZ-1-15	0.0936	0.0016	576.6	9.5	0.0584	0.0006	547	13
LKZ-1-16	0.0927	0.0008	571.2	4.8	0.0588	0.0006	561	14
LKZ-1-17	0.0923	0.0009	569.0	5.5	0.0592	0.0005	577	10
LKZ-1-18	0.0932	0.0009	574.4	5.2	0.0591	0.0005	565	10
LKZ-1-19	0.0928	0.0008	572.0	4.6	0.0585	0.0005	559	9
LKZ-1-20	0.0934	0.0009	575.4	5.1	0.0588	0.0006	554	12
LKZ-1-21	0.0943	0.0015	580.8	8.8	0.0590	0.0011	574	19
LKZ-1-22	0.0927	0.0009	571.6	5.3	0.0591	0.0007	567	14
LKZ-1-23	0.0933	0.0010	575.1	5.9	0.0589	0.0008	573	14
LKZ-1-24	0.0936	0.0012	576.9	7.2	0.0584	0.0007	532	16
LKZ-1-25	0.0933	0.0008	574.7	4.7	0.0587	0.0006	553	13
LKZ-1-26	0.0941	0.0013	579.9	7.5	0.0587	0.0007	563	14
LKZ-1-27	0.0941	0.0013	579.3	7.7	0.0586	0.0005	552	12
LKZ-1-28	0.0939	0.0015	578.5	9.0	0.0583	0.0006	544	14
LKZ-1-29	0.0938	0.0015	577.6	8.9	0.0583	0.0006	541	12
LKZ-1-30	0.0941	0.0014	579.9	8.1	0.0588	0.0007	547	14

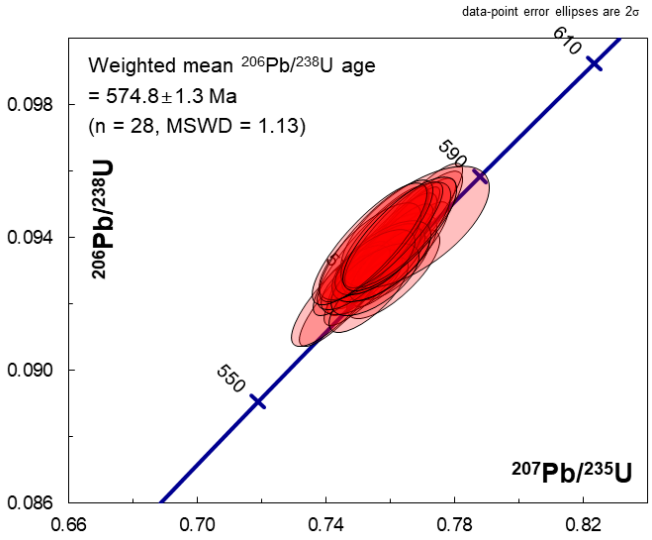

Figure 3. $^{206}Pb/^{238}U$–$^{207}Pb/^{235}U$ concordia diagram showing LA-MC-ICPMS results for the LKZ-1 zircon with ±2σ error ellipses.

Four U-Pb ID-TIMS zircon analyses produced two overlapping, concordant results and two that were slightly discordant (1.2%), but within error of the concordant results (Table 4, Figure 4). Four U-Pb data together yielded a weighted mean $^{207}Pb/^{206}Pb$ age of 575.22 ± 0.98 Ma (MSWD = 0.16, probability = 0.92). The weighted mean $^{206}Pb/^{238}U$ age of the four data was 570.0 ± 2.5 Ma (MSWD = 5.4, probability = 0.001), but if only the two concordant results are considered, a more precise ^{206}Pb-^{238}U

age of 571.7 ± 1.1 Ma is obtained. The Th/U ratios (0.148 ± 0.001) were consistent with those from the SHRIMP analyses (0.146 ± 0.002). The ID-TIMS results may indicate that discordant parts remained in the analyzed fragments in spite of thermal annealing and chemical etching. The discordance of U–Pb age is not attributable to metamictization because the U contents and $^{206}Pb/^{238}U$ dates of the SHRIMP spots did not show any particular trend (Figure S1). If the discordance of our ID-TIMS ages reflects the thermal disturbance experienced by LKZ-1, then the concordance of SHRIMP U–Pb dates may have been caused by the selective analysis of inner, unaffected parts of the crystal. The SEM observation was not helpful to identify the discordant parts because the fragments appeared homogeneous in CL and BSE (Figure 1).

Table 4. U–Pb isotopic data for the LKZ-1 zircon obtained by ID-TIMS.

No.	Weight (mg)	U (ppm)	Th/U	Pbc (pg)	$^{206}Pb/^{204}Pb$	$^{207}Pb/^{235}U$	2σ	$^{206}Pb/^{238}U$	2σ	Error Corr.
sk40p10	0.151	464	0.149	1.4	292650	0.7524	0.0026	0.09216	0.00029	0.976
sk40p11	0.165	494	0.147	2.0	238760	0.7571	0.0019	0.09273	0.00020	0.959
sk40p12	0.101	818	0.147	4.7	104445	0.7583	0.0049	0.09286	0.00057	0.935
sk40p42	0.060	183	0.150	0.5	118809	0.7540	0.0018	0.09232	0.00017	0.925

No.	$^{207}Pb/^{206}Pb$	2σ	$^{206}Pb/^{238}U$ Age (Ma)	2σ	$^{207}Pb/^{235}U$ Age (Ma)	2σ	$^{207}Pb/^{206}Pb$ Age (Ma)	2σ	Disc. %
sk40p10	0.059212	0.000046	568.31	1.74	569.63	1.51	574.90	1.67	1.2
sk40p11	0.059218	0.000045	571.64	1.17	572.34	1.10	575.13	1.66	0.6
sk40p12	0.059224	0.000136	572.43	3.35	573.02	2.84	575.34	5.00	0.5
sk40p42	0.059237	0.000056	569.23	1.00	570.55	1.01	575.81	2.04	1.2

Pbc is total common Pb, and assumes all has laboratory blank isotopic composition; Error Corr. is correlation coefficients of X-Y errors on the concordia plot; Disc. is percent discordance for the given $^{207}Pb/^{206}Pb$ age.

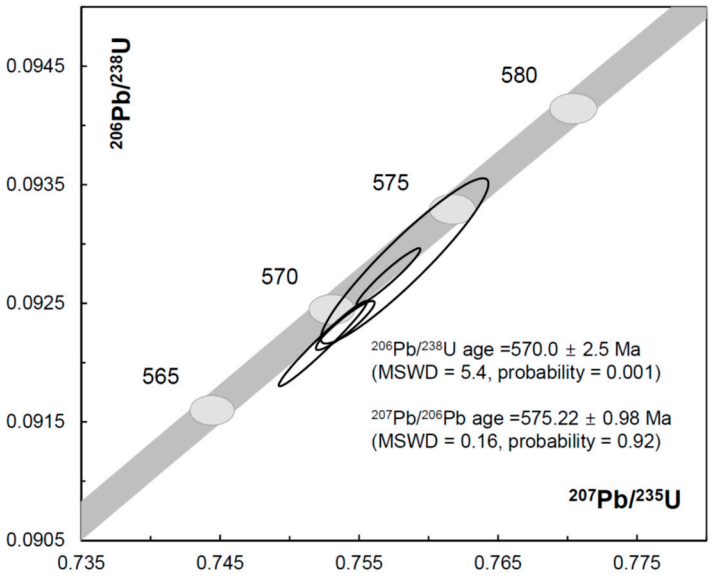

Figure 4. Concordia diagram showing U–Pb data obtained by ID-TIMS analysis of LKZ-1 zircon with ±2σ error ellipses. The concordia curve is depicted as a band, which incorporates the uncertainty of the U decay constants.

In fact, zircon megacrysts commonly show U–Pb age discordance [6]. The discordancy is typically small. For example, the ID-TIMS results for the 91500 zircon reported by Wiedenbeck et al. (1995) [15] were ~0.3% discordant ($^{207}Pb/^{206}Pb$ age = 1065.4 ± 0.3 Ma, $^{206}Pb/^{238}U$ age = 1062.4 ± 0.4 Ma). The ID-TIMS results for SL13, listed by Claoué-Long et al. (1995) [43], were also discordant. The weighted mean $^{207}Pb/^{206}Pb$ and $^{206}Pb/^{238}U$ ages were 576.3 ± 0.8 Ma and 572.1 ± 0.4 Ma, respectively. The discordance of SL13 data was attributed to the extraneous addition of ^{231}Pa into the crystal or uncertainties of the U decay constants [44,45]. The identical U–Pb ages of the SL13 and LKZ-1 zircons may represent an important geologic event in Sri Lanka.

We conclude that the best $^{206}Pb/^{238}U$ ratio of LKZ-1 is equivalent to the SHRIMP age (572.6 ± 2.0 Ma), considering that discordant parts in the zircon fragments may have been included in the ID-TIMS analyses. As stated earlier, this age is consistent with the ID-TIMS $^{206}Pb/^{238}U$ age constrained by concordant results (571.7 ± 1.1 Ma).

3.2. O and Lu–Y–Hf Isotopic Compositions

The O and Lu–Yb–Hf isotopic compositions of LKZ-1 are presented in Tables 5 and 6, respectively. The $\delta^{18}O_{V\text{-}SMOW}$ value of LKZ-1 measured by the laser fluorination system was 10.72 ± 0.02 ‰. The oxygen yield of LKZ-1 was 97.8%, meaning that almost all the oxygen was released from the sample. Thus, any kinetic isotopic fractionation effect caused by incomplete fluorination of sample can be ignored.

Table 5. HR-SIMS O isotopic results for the LKZ-1 zircon.

Spot No.	$\delta^{18}O_{V\text{-}SMOW}$ (‰)	2SE	Spot No.	$\delta^{18}O_{V\text{-}SMOW}$ (‰)	2SE
LKZ-1@1	10.58	0.18	LKZ-1@11	10.77	0.19
LKZ-1@2	10.79	0.28	LKZ-1@12	10.88	0.22
LKZ-1@3	10.52	0.25	LKZ-1@13	10.48	0.21
LKZ-1@4	10.37	0.34	LKZ-1@14	10.68	0.12
LKZ-1@5	10.59	0.43	LKZ-1@15	10.63	0.29
LKZ-1@6	10.60	0.33	LKZ-1@16	10.62	0.28
LKZ-1@7	10.96	0.28	LKZ-1@17	10.54	0.23
LKZ-1@8	10.60	0.45	LKZ-1@18	10.81	0.31
LKZ-1@9	10.56	0.32	LKZ-1@19	10.74	0.17
LKZ-1@10	10.69	0.23	LKZ-1@20	10.56	0.31
			Average	10.65	
			SD	0.14	

Laser fluorination value = 10.72 ± 0.02‰ (1SD).

During the analytical session at the CAS, the 91500 and Penglai [46] zircons yielded an average measured $\delta^{18}O_{V\text{-}SMOW}$ value of 15.16 ± 0.17 ‰ and 10.40 ± 0.21‰, respectively. Detailed data, including ^{16}O intensities, $^{18}O/^{16}O$ ratios, and spot locations on the mount, are given in Table S2. The interlaboratory calibration work of Wiedenbeck et al. (2004) for the 91500 zircon [47] reported laser fluorination $\delta^{18}O_{V\text{-}SMOW}$ values between 10.07‰ and 9.74‰. Although the simple mean was 9.86 ± 0.11‰ (n = 13), the high-end value (10.07‰) was preferred in this study to correct the IMF because the simple mean yielded a slightly underestimated $\delta^{18}O_{V\text{-}SMOW}$ average (5.08‰) for the Penglai zircon (laser fluorination $\delta^{18}O_{V\text{-}SMOW}$ = 5.31 ± 0.12‰; [46]). An IMF value of –5.09‰, with reference to the 91500 zircon value of 10.07‰, generated an average $\delta^{18}O_{V\text{-}SMOW}$ value of 10.65 ± 0.14‰ for the LKZ-1 zircon (Figure 5). This value was indistinguishable from that obtained by the laser fluorination method (10.72 ± 0.02‰). The Penglai zircon measured during several analytical sessions yielded an IMF-corrected $\delta^{18}O_{V\text{-}SMOW}$ of 5.29 ± 0.34 ‰ (n = 23) (Table S2).

Table 6. LA-MC-ICPMS Lu–Yb–Hf results for the LKZ-1 zircon.

Spot No.	$^{176}Hf/^{177}Hf$	2SE (ppm)	$^{178}Hf/^{177}Hf$	2SE (ppm)	$^{176}Lu/^{177}Hf$	2SE (%)	$^{176}Yb/^{177}Hf$	2SE (%)	$\varepsilon_{Hf}(0)$	$\varepsilon_{Hf}(t)$
LKZ-1	0.281788	92	1.467234	45	0.000104	0.13	0.00394	0.64	−34.8	−22.3
LKZ-2	0.281816	89	1.467252	53	0.000104	0.12	0.00392	0.61	−33.8	−21.3
LKZ-3	0.281776	96	1.467270	75	0.000102	0.14	0.00388	0.62	−35.2	−22.7
LKZ-4	0.281805	82	1.467186	57	0.000104	0.13	0.00394	0.56	−34.2	−21.7
LKZ-5	0.281808	85	1.467226	48	0.000104	0.12	0.00395	0.63	−34.1	−21.6
LKZ-6	0.281800	85	1.467237	42	0.000104	0.12	0.00393	0.61	−34.4	−21.8
LKZ-7	0.281803	92	1.467215	51	0.000103	0.13	0.00393	0.64	−34.3	−21.7
LKZ-8	0.281785	89	1.467261	50	0.000104	0.13	0.00392	0.61	−34.9	−22.4
LKZ-9	0.281777	92	1.467226	58	0.000104	0.13	0.00393	0.61	−35.2	−22.6
LKZ-10	0.281779	82	1.467236	55	0.000104	0.14	0.00393	0.54	−35.1	−22.6
LKZ-11	0.281789	92	1.467268	55	0.000103	0.16	0.00376	0.48	−34.8	−22.2
LKZ-12	0.281796	96	1.467236	57	0.000106	0.17	0.00393	0.46	−34.5	−22.0
LKZ-13	0.281797	92	1.467261	61	0.000103	0.16	0.00379	0.45	−34.5	−21.9
LKZ-14	0.281805	96	1.467233	51	0.000106	0.18	0.00397	0.53	−34.2	−21.7
LKZ-15	0.281792	96	1.467264	65	0.000103	0.15	0.00383	0.47	−34.7	−22.1
LKZ-16	0.281815	85	1.467229	44	0.000103	0.14	0.00391	0.59	−33.8	−21.3
LKZ-17	0.281807	82	1.467233	51	0.000104	0.12	0.00392	0.54	−34.1	−21.6
LKZ-18	0.281790	89	1.467161	59	0.000104	0.14	0.00397	0.55	−34.7	−22.2
LKZ-19	0.281793	89	1.467256	57	0.000103	0.13	0.00392	0.61	−34.6	−22.1
LKZ-20	0.281811	85	1.467302	62	0.000104	0.14	0.00394	0.58	−34.0	−21.4
LKZ-21	0.281805	99	1.467251	50	0.000102	0.17	0.00377	0.50	−34.2	−21.7
LKZ-22	0.281773	89	1.467230	52	0.000103	0.15	0.00381	0.47	−35.3	−22.8
LKZ-23	0.281792	89	1.467250	52	0.000102	0.16	0.00381	0.55	−34.7	−22.1
LKZ-24	0.281772	99	1.467269	55	0.000102	0.16	0.00377	0.53	−35.4	−22.8
LKZ-25	0.281779	85	1.467225	52	0.000102	0.15	0.00385	0.65	−35.1	−22.6
LKZ-26	0.281775	106	1.467352	44	0.000105	0.21	0.00310	0.52	−35.3	−22.7
LKZ-27	0.281756	99	1.467289	42	0.000107	0.20	0.00320	0.50	−35.9	−23.4
LKZ-28	0.281805	92	1.467365	39	0.000104	0.19	0.00318	0.47	−34.2	−21.7
LKZ-29	0.281795	103	1.467350	44	0.000104	0.19	0.00320	0.50	−34.6	−22.0
LKZ-30	0.281825	103	1.467347	44	0.000104	0.19	0.00323	0.50	−33.5	−21.0
LKZ-31	0.281798	117	1.467337	48	0.000104	0.21	0.00318	0.53	−34.4	−21.9
LKZ-32	0.281787	103	1.467351	44	0.000103	0.20	0.00318	0.53	−34.8	−22.3
LKZ-33	0.281787	103	1.467360	42	0.000105	0.19	0.00324	0.49	−34.8	−22.3
LKZ-34	0.281787	110	1.467324	46	0.000101	0.23	0.00307	0.59	−34.8	-22.3
LKZ-35	0.281791	106	1.467343	40	0.000105	0.21	0.00321	0.56	−34.7	−22.2
LKZ-36	0.281793	103	1.467316	44	0.000103	0.23	0.00318	0.57	−34.6	−22.1
LKZ-37	0.281815	106	1.467329	41	0.000104	0.23	0.00321	0.56	−33.8	−21.3
LKZ-38	0.281805	103	1.467327	42	0.000108	0.24	0.00334	0.54	−34.2	−21.7
LKZ-39	0.281821	96	1.467361	42	0.000106	0.21	0.00328	0.55	−33.6	−21.1
LKZ-40	0.281799	131	1.467363	40	0.000106	0.21	0.00328	0.61	−34.4	−21.9
LKZ-41	0.281838	106	1.467339	36	0.000105	0.20	0.00327	0.55	−33.0	−20.5
LKZ-42	0.281789	117	1.467322	42	0.000103	0.23	0.00315	0.60	−34.8	−22.2
LKZ-43	0.281771	114	1.467375	40	0.000101	0.26	0.00311	0.64	−35.4	−22.9
LKZ-44	0.281777	124	1.467349	36	0.000104	0.23	0.00320	0.63	−35.2	−22.7
LKZ-45	0.281785	131	1.467365	41	0.000101	0.21	0.00315	0.64	−34.9	−22.4
Average	0.281794		1.467286		0.000104		0.00358		−34.6	−22.0
SD	0.000016		0.000057		0.000001		0.00035		0.6	0.6

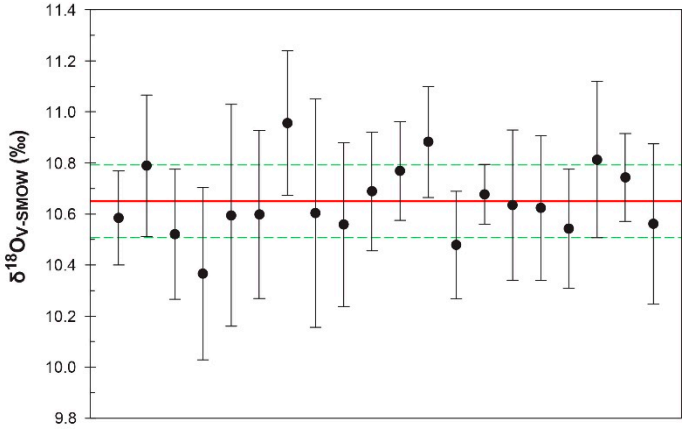

Figure 5. O isotopic variation in the LKZ-1 zircon based on HR-SIMS analyses. Vertical error bars denote 2 standard errors. Solid and dashed lines represent the average (10.65‰) and standard deviation (±0.14‰), respectively.

The LA-MC-ICPMS analyses produced an average $^{176}Hf/^{177}Hf$ of 0.282294 ± 0.000021 (n = 41) for the 91500 zircon (Table S3), which was consistent with the MC-ICPMS result obtained by solution chemistry (0.282308 ± 0.000006; [48]). The $^{176}Lu/^{177}Hf$ results (0.00028 ± 0.00010) for the 91500 zircon

(Table S3) were also consistent with the solution chemistry-based data (0.00031 ± 0.00007; [48]). The LKZ-1 zircon showed little intra- and inter-grain variation in $^{176}Hf/^{177}Hf$ (0.281794 ± 0.000016; Figure 6), $^{176}Lu/^{177}Hf$ (0.000104 ± 0.000001), and $^{176}Yb/^{177}Hf$ (0.00358 ± 0.00035) (n = 45). The $^{178}Hf/^{177}Hf$ ratios were indistinguishable between 91500 (1.467289 ± 0.000059) and LKZ-1 (1.467286 ± 0.000057), with their $^{176}Lu/^{177}Hf$ and $^{176}Yb/^{177}Hf$ ratios showing a good positive correlation (R^2 = 0.97). The initial ε_{Hf} values calculated from the $^{176}Hf/^{177}Hf$ and $^{176}Lu/^{177}Hf$ ratios and SHRIMP $^{206}Pb/^{238}U$ age (572.6 Ma) varied narrowly and gave an average value of –22.0 ± 0.6. The $^{176}Hf/^{177}Hf$ and $^{176}Lu/^{177}Hf$ ratios did not show a clear trend (Figure S2).

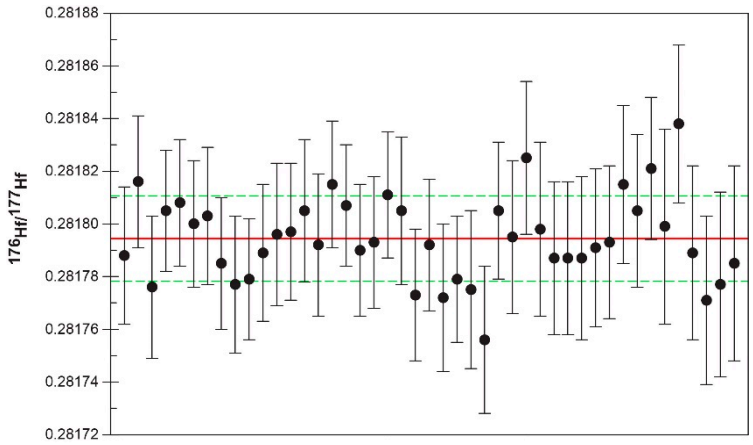

Figure 6. Hafnium isotopic variation in the LKZ-1 zircon. Vertical error bars denote 2 standard errors. Solid and dashed lines represent the average (0.281794) and standard deviation (±0.000016), respectively.

3.3. Chemical Composition

The LA-quadrupole ICPMS results for the 91500 and LKZ-1 zircons are summarized in Table 7 with literature data [15,47,49–51]. The individual spot data analysed in this study are listed in Table S4.

Table 7. Summary of chemical data for the 91500 and LKZ-1 zircons (unit: ppm).

	91500													LKZ-1			
	[15,47]			[49]			[50]			[51]			This Study	SD (n = 37)	This Study	SD (n = 28)
P	35	±	17										14	7	17	8
Ca													102	66	68	50
Y	153	±	14	147	±	22							148	36	86	6
La	0.013	±	0.01	<0.08	±	0.05	0.014	±	0.011	0.031	±	0.038	0.013	0.025	0.003	0.002
Ce	2.56	±	0.20	2.5	±	0.5	2.59	±	0.43	2.77	±	0.41	2.19	0.34	0.84	0.08
Pr	0.020	±	0.01	<0.05	±	0.05	0.035	±	0.015	0.022	±	0.021	0.019	0.027	0.015	0.012
Nd	0.25	±	0.01	<0.35	±	0.07	0.295	±	0.064	0.324	±	0.085	0.25	0.14	0.15	0.05
Sm	0.38	±	0.03	0.41	±	0.2	0.278	±	0.084	0.624	±	0.246	0.52	0.24	0.29	0.08
Eu	0.19	±	0.02	0.37	±	0.17	0.191	±	0.065	0.310	±	0.112	0.26	0.11	0.09	0.03
Gd	1.76	±	0.39	2.1	±	0.35	1.60	±	0.39	2.719	±	0.658	2.50	0.90	1.53	0.17
Tb	0.78	±	0.12				0.75	±	0.20	1.11	±	0.25	0.94	0.31	0.61	0.06
Dy	10.3	±	0.9	12	±	2.1	12.3	±	2.5	14.2	±	2.5	11.8	3.4	7.3	0.6
Ho	4.60	±	0.46	4.9	±	0.7	5.1	±	1.4	5.83	±	0.90	4.92	1.37	2.93	0.26
Er	23.7	±	2.6	26	±	3.6	28.6	±	6.2	28.2	±	4.6	27.1	7.0	15.3	1.2
Tm	5.95	±	0.71				7.5	±	1.8	8.44	±	1.27	6.81	1.63	3.44	0.32
Yb	60.1	±	8.4	66	±	7.3	77	±	18	101	±	16	69	17	32	3
Lu	14.1	±	1.7	14	±	1.9	17.1	±	3.8	13.9	±	2.0	13.8	3.1	5.9	0.5
Hf	5895			6400	±	900							5780	340	7740	310
Th	28.61	±	0.07	31	±	4.9							30	6	94	6
U	81.2			88	±	15							83	14	654	31

For LKZ-1, U and Th concentrations were normalized by ^{29}Si. All the other elements were normalized by ^{91}Zr. [15]; ID-TIMS results (Hf, Th, U), [47]; P, EPMA result. Y and REE concentrations are working values from inter-laboratory SIMS analyses. [49,51]; LA-ICPMS results, [50]; HR-SIMS results.

For the 91500 zircon, the internal normalization by ^{91}Zr generated concentration results close to the literature data, except for U and Th. We employed ^{29}Si-normalization for the calculation of U and Th concentrations because the ^{91}Zr-normalization for these elements yielded results consistently ~15% lower than the recommended values. The ^{29}Si-normalized results for U (83 ± 14 ppm) and Th

(30 ± 6 ppm), and the ^{91}Zr-normalized result for Hf (5780 ± 340 ppm) agreed well with the ID-TIMS data ([U] = 81.2 ppm, [Th] = 28.61 ppm, [Hf] = 5895 ppm; [15]). The ^{91}Zr-normalized results for P (14 ± 7 ppm) and Y (148 ± 36 ppm) were marginally or closely similar to the literature data [[P] = 35 ± 17 ppm, [Y] = 153 ± 14 ppm; [47]). As shown in Figure 7a, the chondrite-normalized pattern of our ^{91}Zr-normalized rare earth element (REE) data generally matched the recommended values. The slightly negative Eu anomalies in our data (Eu/Eu* = 0.72 ± 0.17) are consistent with the data previously obtained by inter-laboratory SIMS analyses [47].

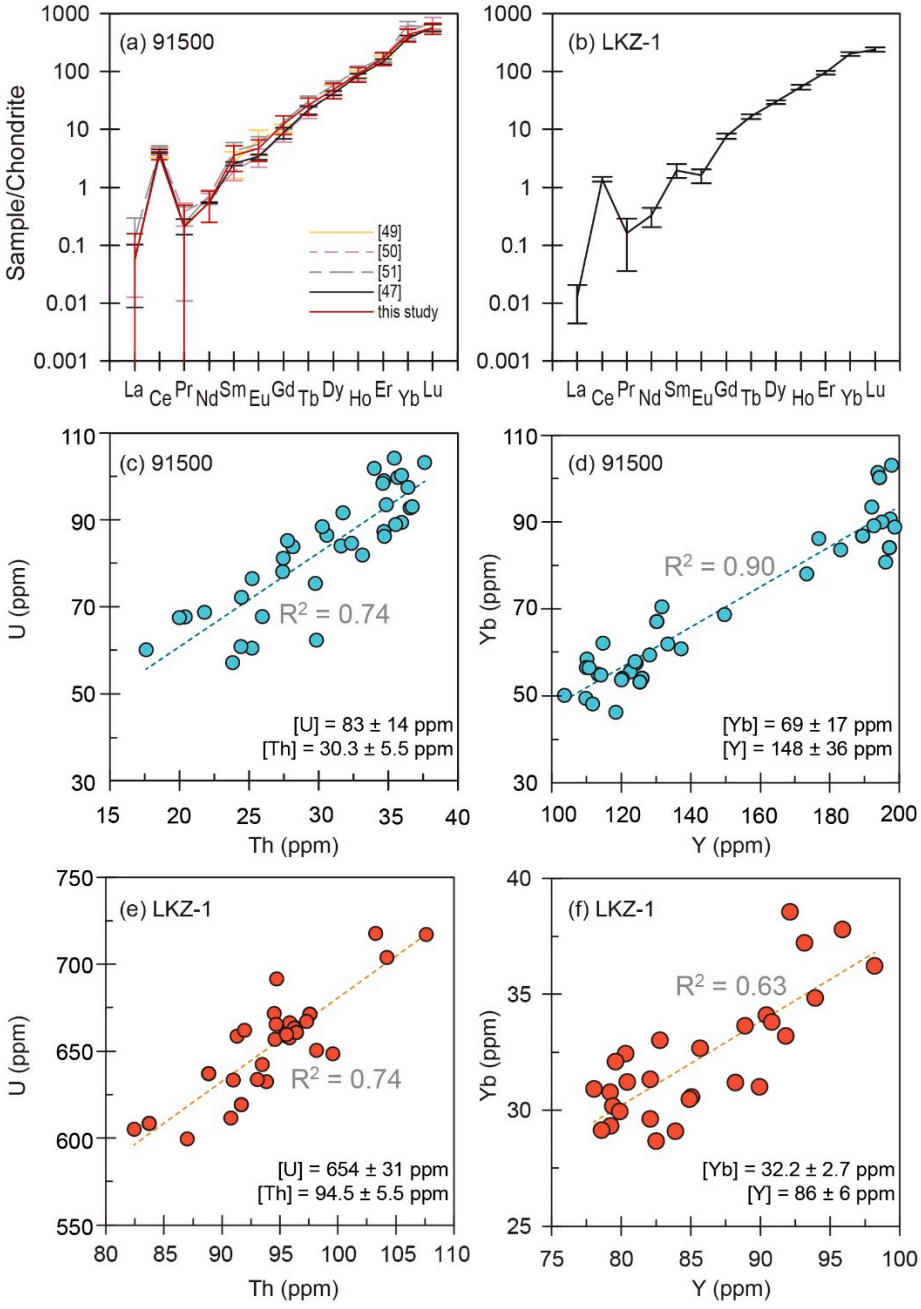

Figure 7. Chondrite-normalized REE patterns of 91500 (**a**) and LKZ-1 (**b**) zircons. Chondrite values were taken from McDonough and Sun (1995) [52]. Vertical error bars denote 1 standard deviation of our data, or uncertainties reported in previous works. (**c**–**f**) U vs. Th and Yb vs. Y variations for 91500 and LKZ-1 zircons.

For most elements >1 ppm, the relative standard deviation values for the concentration data for the LKZ-1 zircon were <10%. The chondrite-normalized REE pattern of LKZ-1 (Figure 7b) was highly consistent, with prominently positive Ce (Ce/Ce^* = 44 ± 32) and negative Eu (Eu/Eu^* = 0.43 ± 0.17) anomalies. The ratios between the heavy and middle REEs were also consistent ($(Lu/Gd)_N$ = 31 ± 3). The U (654 ± 31 ppm) and Th (94 ± 6 ppm) concentrations, and their ratios (Th/U = 0.144 ± 0.004), were comparable to the SHRIMP results. The positive correlations observed between U and Th concentrations and Yb and Y concentrations (Figure 7c–f) indicate that our data reflect inter- and intra-grain chemical variation, rather than random analytical errors.

4. Conclusions

The results of our ID-TIMS, HR-SIMS, and LA-MC-ICPMS analyses demonstrate that the LKZ-1 zircon is nearly concordant in U–Pb age, with negligible common Pb content and a consistent Th/U ratio. LKZ-1 is fairly homogeneous in O–Hf isotopic and chemical composition. These consistencies suggest that LKZ-1 can be used as a suitable working standard for geochronological and isotopic/geochemical analyses. Fragments of the LKZ-1 zircon are available upon request from the lead author of this paper.

Supplementary Materials: The following are available online at http://www.mdpi.com/2075-163X/9/5/325/s1, Figure S1: Plot of $^{206}Pb/^{238}U$ dates and U concentrations for the SHRIMP spots of the LKZ-1 zircon. Figure S2: $^{176}Hf/^{177}Hf$ vs. $^{176}Lu/^{177}Hf$ plot for the LKZ-1 zircon. Table S1: SHRIMP U–Th–Pb results for the Plešovice zircon. Table S2: HR-SIMS (Cameca 1280) oxygen isotope data for the analyzed zircons. Table S3: LA-MC-ICPMS Lu–Yb–Hf isotopic results for the 91500 zircon. Table S4: LA-ICPMS results for the 91500 and LKZ-1 zircons.

Author Contributions: Conceptualization, A.C.-s.C.; methodology, Y.-J.J., S.L., K.Y., H.J.J., H.-S.L., C.P., N.K.K., X.-H.L. and S.L.K.; compiling and writing of the manuscript, A.C.-s.C.

Funding: This research was supported by a Korea Basic Science Institute grant (C39709) and a National Research Foundation of Korea grant funded by the government of Korea's Ministry of Science and ICT (2016R1A2B4007283), awarded to A.C.C.

Acknowledgments: We are grateful for the assistance of Sook Ju Kim, Seon Gyu Kim, and Guo-Qiang Tang in the laboratory work. Insightful reviews by the editor and three anonymous journal reviewers improved the manuscript substantially.

Conflicts of Interest: The funders had no role in the design of the study; in the collection, analyses, or interpretation of data; in the writing of the manuscript, or in the decision to publish the results.

References

1. Jeffery, P.G.; Hutchison, D. *Chemical Methods of Rock Analysis*, 3rd ed.; Pergamon Press: Oxford, UK, 1981; p. 379.
2. Potts, P.J. *Handbook of Rock Analysis*; Viridian Publishing: Surrey, UK, 2003; p. 622.
3. Bardo, J.; Ryerson, F.J.; Weber, P.K.; Ricolleau, A.; Fallon, S.J.; Hutcheon, I.D. Chemical imaging with NanoSIMS: A window into deep-Earth geochemistry. *Earth Planet. Sci. Lett.* **2007**, *262*, 543–551.
4. Valley, J.W.; Cavosie, A.J.; Ushikubo, T.; Reinhard, D.A.; Lawrence, D.F.; Larson, D.J.; Clifton, P.H.; Kelly, T.F.; Wilde, S.A.; Moser, D.E.; et al. Hadean age for a post-magma-ocean zircon confirmed by atom-probe tomography. *Nat. Geosci.* **2014**, *7*, 219–223. [CrossRef]
5. Davidson, J.P.; Morgan, D.J.; Charlier, B.L.A.; Harlou, R.; Hora, J.M. Microsampling and isotopic analysis of igneous rocks: Implications for the study of magmatic systems. *Annu. Rev. Earth Planet. Sci.* **2007**, *35*, 273–311. [CrossRef]
6. Ireland, T.R.; Williams, I.S. Considerations in zircon geochronology by SIMS. *Rev. Mineral. Geochem.* **2003**, *53*, 215–241. [CrossRef]
7. Valley, J.W. Oxygen isotopes in zircon. *Rev. Mineral. Geochem.* **2003**, *53*, 343–385. [CrossRef]
8. Košler, J.; Sylvester, P.J. Present trends and the future of zircon in geochronology: Laser ablation ICP-MS. *Rev. Mineral. Geochem.* **2003**, *53*, 243–275. [CrossRef]
9. Yokoyama, T.D.; Suzuki, T.; Kon, Y.; Hirata, T. Determinations of rare earth element abundance and U-Pb age of zircons using multisport laser ablation-inductively coupled plasma mass spectrometry. *Anal. Chem.* **2011**, *83*, 8892–8899. [CrossRef] [PubMed]

10. Cherniak, D.J.; Watson, B. Diffusion in zircon. *Rev. Mineral. Geochem.* **2003**, *53*, 113–143. [CrossRef]
11. Hawkesworth, C.J.; Kemp, A.I.S. Using hafnium and oxygen isotopes in zircons to unravel the record of crustal evolution. *Chem. Geol.* **2006**, *226*, 144–162. [CrossRef]
12. Kemp, A.I.S.; Hawkesworth, C.J.; Paterson, B.A.; Kinny, P.D. Episodic growth of the Gondwana supercontinent from hafnium and oxygen isotopes in zircon. *Nature* **2006**, *439*, 580–583. [CrossRef]
13. Jo, H.J.; Cheong, A.C.S.; Ryu, J.S.; Kim, N.; Yi, K.; Jung, H.; Li, X.H. In situ oxygen isotope records of crustal self-cannibalization selectively captured by zircon crystals from high-δ^{26}Mg granitoids. *Geology* **2016**, *44*, 339–342. [CrossRef]
14. Grimes, C.B.; John, B.E.; Kelemen, P.B.; Mazdab, F.K.; Wooden, J.L.; Cheadle, M.J.; Hanghøj, K.; Schwartz, J.J. Trace element chemistry of zircons from oceanic crust: A method for distinguishing detrital zircon provenance. *Geology* **2007**, *35*, 643–646. [CrossRef]
15. Wiedenbeck, M.; Allé, P.; Corfu, F.; Griffin, W.L.; Meier, M.; Oberli, F.; von Quadt, A.; Roddick, J.C.; Speigel, W. Three natural zircon standards for U-Th-Pb, Lu-Hf, trace element and REE analyses. *Geostand. Newslett.* **1995**, *19*, 1–23. [CrossRef]
16. Paces, J.B.; Miller, J.D., Jr. Precise U–Pb ages of Duluth Complex and related mafic intrusions, Northeastern Minnesota: geochronological insights to physical, petrogenic, paleomagnetic, and tectonomagmatic processes associated with the 1.1 Ga midcontinent rift system. *J. Geophys. Res.* **1993**, *98*, 13997–14013. [CrossRef]
17. Black, L.P.; Kamo, S.L.; Allen, C.M.; Aleinikoff, J.N.; Davis, D.W.; Korsch, R.J.; Foudoulis, C. TEMORA 1: A new zircon standard for Phanerozoic U–Pb geochronology. *Chem. Geol.* **2003**, *200*, 155–170. [CrossRef]
18. Black, L.P.; Kamo, S.L.; Allen, C.M.; Davis, D.W.; Aleinikoff, J.N.; Valley, J.W.; Mundil, R.; Campbell, I.H.; Korsch, R.J.; Williams, I.S.; et al. Improved ^{206}Pb/^{238}U microprobe geochronology by the monitoring of a trace-element-related matrix effect; SHRIMP, ID-TIMS, ELA-ICP-MS and oxygen isotope documentation for a series of zircon standards. *Chem. Geol.* **2004**, *205*, 115–140. [CrossRef]
19. Sláma, J.; Košler, J.; Condon, D.J.; Crowley, J.L.; Gerdes, A.; Hanchar, J.M.; Horstwood, M.S.A.; Morris, G.A.; Nasdala, L.; Norberg, N.; et al. Plešovice zircon—A new natural reference material for U-Pb and Hf isotopic microanalysis. *Chem. Geol.* **2008**, *249*, 1–35. [CrossRef]
20. Takehara, M.; Horie, K.; Hokada, T.; Kiyokawa, S. New insight into disturbance of U-Pb and trace-element systems in hydrothermally altered zircon via SHRIMP analyses of zircon from the Duluth Gabbro. *Chem. Geol.* **2018**, *484*, 168–178. [CrossRef]
21. Jeong, Y.J.; Lee, S.; Kim, S.J.; Jo, H.J.; Yi, K.; Cheong, A.C.S. U–Th isotopic microanalysis of zircon reference materials and KBSI working standards. *J. Anal. Sci. Technol.* **2018**, *9*, 16. [CrossRef]
22. Kim, S.J.; Lee, T.H.; Yi, K.; Jeong, Y.J.; Cheong, C.S. Characterization of new zircon and monazite working standards LKZ-1, BRZ-1, COM-1 and BRM-1. In Proceedings of the 1st Japan-Korea SHRIMP meeting, Higashi-Hiroshima, Japan, 14–16 September 2015.
23. Williams, I.S. U-Th-Pb geochronology by ion microprobe. In *Applications of Microanalytical Techniques to Understanding Mineralizing Processes*; McKibben, M.A., Shanks, W.C., III, Rindley, W.I., Eds.; Society of Economic Geologists: Littleton, CO, USA, Reviews in Economic Geology; 1998; Volume 7, pp. 1–35.
24. Ludwig, K.R. *User's manual for Squid 2.50*; Berkeley Geochronology Center: Berkeley, CA, USA, Special Publication No. 5; 2009; 110p.
25. Ludwig, K.R. *User's manual for Isoplot 3.6: A geochronological toolkit for Microsoft Excel*; Berkeley Geochronology Center: Berkeley, CA, USA, Special Publication No. 4; 2008; 77p.
26. Mattinson, J.M. Zircon U-Pb chemical abrasion ("CA-TIMS") method: Combined annealing and multi-step partial dissolution analysis for improved precision and accuracy of zircon ages. *Chem. Geol.* **2005**, *220*, 47–66. [CrossRef]
27. Krogh, T.E. A low contamination method for hydrothermal decomposition of zircon and extraction of U and Pb for isotopic age determinations. *Geochim. Cosmochim. Acta* **1973**, *37*, 485–494. [CrossRef]
28. Gerstenberger, H.; Haase, G. A highly effective emitter substance for mass spectrometric Pb isotope ratio determinations. *Chem. Geol.* **1997**, *136*, 309–312. [CrossRef]
29. Jaffey, A.H.; Flynn, K.F.; Glendenin, L.E.; Bentley, W.C.; Essling, A.M. Precision measurement of half-lives and specific activities of ^{235}U and ^{238}U. *Phys. Rev.* **1971**, *4*, 1889–1906.
30. Ludwig, K.R. *User's manual for Isoplot 3.00: A geochronological toolkit for Microsoft Excel*; Berkeley Geochronology Center: Berkeley, CA, USA, Special Publication No. 4; 2003; p. 71.

31. Kim, N.K.; Kusakabe, M.; Park, C.; Lee, J.I.; Nagao, K.; Enokido, Y.; Yamashita, S.; Park, S.Y. An automated laser fluorination technique for high-precision analysis of three oxygen isotopes in silicates. *Rapid Commun. Mass Sp.* **2019**, *33*, 641–649. [CrossRef] [PubMed]
32. Baertschi, P. Absolute ^{18}O content of Standard Mean Ocean Water. *Earth Planet. Sci. Lett.* **1976**, *31*, 341–344. [CrossRef]
33. Paton, C.; Hellstrom, J.; Paul, B.; Woodhead, J.; Hergt, J. Iolite: freeware for the visualisation and processing of mass spectrometric data. *J. Anal. At. Spectrom.* **2011**, *26*, 2508–2518. [CrossRef]
34. Chu, N.C.; Taylor, R.N.; Chavagnac, V.; Nesbitt, R.W.; Boella, M.; Milton, J.A. Hf isotope ratio analysis using multi-collector inductively coupled plasma mass spectrometry: An evaluation of isobaric interference corrections. *J. Anal. At. Spectrom.* **2002**, *17*, 1567–1574. [CrossRef]
35. Vervoort, J.D.; Patchett, P.J.; Söderlund, U.; Baker, M. Isotopic composition of Yb and the determination of Lu concentrations and Lu/Hf ratios by isotope dilution using MC-ICPMS. *Geochem. Geophys. Geosyst.* **2004**, *5*, Q11002. [CrossRef]
36. Choi, M.S.; Cheong, C.S.; Kim, J.; Shin, H.S. Hafnium isotope analysis of mixed standard solutions by multi-collector inductively coupled plasma mass spectrometry: an evaluation of isobaric interference corrections. *J. Anal. Sci. Technol.* **2013**, *4*, 1. [CrossRef]
37. Iizuka, T.; Hirata, T. Improvements of precision and accuracy in in-situ Hf isotope microanalysis of zircon using the laser ablation-MC-ICPMS technique. *Chem. Geol.* **2005**, *220*, 121–137. [CrossRef]
38. Scherer, E.; Münker, C.; Mezger, K. Calibration of the lutetium-hafnium clock. *Science* **2001**, *293*, 683–687. [CrossRef] [PubMed]
39. Blichert-Toft, J.; Albarède, F. The Lu-Hf isotope geochemistry of chondrites and the evolution of the mantle-crust system. *Earth Planet. Sci. Lett.* **1997**, *148*, 243–258. [CrossRef]
40. Guillong, M.; Günther, D. Effect of particle size distribution on ICP-induced elemental fractionation in laser ablation-inductively coupled plasma-mass spectrometry. *J. Anal. At. Spectrom.* **2002**, *17*, 831–837. [CrossRef]
41. Jochum, K.P.; Weis, U.; Stoll, B.; Kuzmin, D.; Yang, Q.; Raczek, I.; Jacob, D.E.; Stracke, A.; Birbaum, K.; Frick, D.A.; et al. Determination of reference values for NIST SRM 610-617 glasses following ISO guidelines. *Goestan. Geoanal. Res.* **2011**, *35*, 397–429. [CrossRef]
42. Stacey, J.S.; Kramers, J.D. Approximation of terrestrial lead isotope evolution by a two-stage model. *Earth Planet. Sci. Lett.* **1975**, *26*, 207–221. [CrossRef]
43. Claoué-Long, J.C.; Compston, W.; Roberts, J.; Fanning, C.M. Two Carboniferous ages: A comparison of SHRIMP zircon dating with conventional zircon ages and $^{40}Ar/^{39}Ar$ analysis. In *Geochronology Time Scales and Global Stratigraphic Correlation*; Berggren, W.A., Kent, D.V., Aubrey, M.-P., Hardenbol, J., Eds.; Society for Sedimentary Geology Special Publication: Tulsa, OK, USA, 1995; Volume 54, pp. 3–21.
44. Mattinson, J.M. U–Pb ages of zircons: A basic examination of error propagation. *Chem. Geol.* **1987**, *66*, 151–162. [CrossRef]
45. Black, L.P.; Kamo, S.L.; Williams, I.S.; Mundil, R.; Davis, D.W.; Korsch, R.J.; Foudoulis, C. The application of SHRIMP to Phanerozoic geochronology; a critical appraisal of four zircon standards. *Chem. Geol.* **2003**, *200*, 171–188. [CrossRef]
46. Li, X.H.; Long, W.G.; Li, Q.L.; Liu, Y.; Zheng, Y.F.; Yang, Y.H.; Chamberlain, K.R.; Wan, D.F.; Guo, C.H.; Wang, X.C.; et al. Penglai zircon megacrysts: A potential new working reference microbeam determination of Hf–O isotopes and U–Pb age. *Geostand. Geoanal. Res.* **2010**, *34*, 117–134. [CrossRef]
47. Wiedenbeck, M.; Hanchar, J.M.; Peck, W.H.; Sylvester, P.; Valley, J.; Whitehouse, M.; Kronz, A.; Morishita, Y.; Nasdala, L.; Fiebig, J.; et al. Further characterisation of the 91500 zircon crystal. *Geostand. Geoanal. Res.* **2004**, *28*, 9–39. [CrossRef]
48. Blichert-Toft, J. The Hf isotopic composition of zircon reference material 91500. *Chem. Geol.* **2008**, *253*, 252–257. [CrossRef]
49. Belousova, E.A.; Griffin, W.L.; O'Reilly, S.Y.; Fisher, N.I. Igneous zircon: Trace element composition as an indicator of source rock type. *Contrib. Mineral. Petrol.* **2002**, *143*, 602–622. [CrossRef]
50. Sano, Y.; Terada, K.; Fukuoka, T. High mass resolution ion microprobe analysis of rare earth elements in silicate glass, apatite and zircon: lack of matrix dependency. *Chem. Geol.* **2002**, *184*, 217–230. [CrossRef]

51. Iizuka, T.; Hirata, T. Simultaneous determinations of U–Pb age and REE abundances for zircons using ArF excimer laser ablation-ICPMS. *Geochem. J.* **2004**, *38*, 229–241. [CrossRef]
52. McDonough, W.F.; Sun, S.S. The composition of the Earth. *Chem. Geol.* **1995**, *120*, 223–253. [CrossRef]